

# Evidence for Orbital Decay of RX J1914.4+2456: Gravitational Radiation and the Nature of the X-ray Emission

Tod E. Strohmayer

*Laboratory for High Energy Astrophysics, NASA's Goddard Space Flight Center, Greenbelt,  
MD 20771; stroh@clarence.gsfc.nasa.gov*

## ABSTRACT

RX J1914.4+2456 is a candidate double-degenerate binary (AM CVn) with a putative 569 s orbital period. If this identification is correct, then it has one of the shortest binary orbital periods known, and gravitational radiation should drive the orbital evolution and mass transfer if the binary is semi-detached. Here we report the results of a coherent timing study of the archival ROSAT data for RX J1914.4+2456. We performed a phase coherent timing analysis using all five ROSAT observations spanning an  $\approx 4$  year period. We demonstrate that all the data can be phase connected, and we show that the 1.756 mHz orbital frequency is increasing at a rate of  $1.5 \pm 0.4 \times 10^{-17} \text{ Hz s}^{-1}$ , consistent with the expected loss of angular momentum from the binary system via gravitational radiation. In addition to providing evidence for the emission of gravitational waves, our measurement of the orbital  $\dot{\nu}$  constrains models for the X-ray emission and the nature of the secondary. If stable mass accretion drives the X-ray flux, then a positive  $\dot{\nu}$  is inconsistent with a degenerate donor. A helium burning dwarf is compatible if indeed such systems can have periods as short as that of RX J1914.4+2456, an open theoretical question. Our measurement of a positive  $\dot{\nu}$  is consistent with the unipolar induction model of Wu et al. which does not require accretion to drive the X-ray flux. We discuss how future timing measurements of RX J1914.4+2456 (and systems like it) with for example, Chandra and XMM-Newton, can provide a unique probe of the interaction between mass loss and gravitational radiation. We also discuss the importance of such measurements in the context of gravitational wave detection from space, such as is expected in the future with the LISA mission.

*Subject headings:* Binaries: general - Stars: individual (RX J1914.4+2456) - Stars: white dwarfs - cataclysmic variables - X-rays: stars - X-rays: binaries

## 1. Introduction

The evolution of highly compact binary stars is driven to a large extent by the interplay between loss of angular momentum from gravitational radiation and mass transfer between the components (see, for example Rappaport, Joss & Webbink 1982). Detailed study of the orbital evolution of such systems can thus provide a unique physical laboratory for the study of gravitational radiation and its effect on binary evolution.

The shortest period cataclysmic variables (CVs), the AM CVn stars, are the most compact binaries known, with orbital periods  $< 40$  minutes. Many may be double-degenerate systems (see Warner 1995 for a review). Their formation is complex, depending on unstable mass transfer leading to common envelope (CE) evolution, processes which are not well understood (see Nelemans et al. 2001). Such systems likely begin as a pair of main sequence stars, each of  $3 - 5 M_{\odot}$ . After perhaps two episodes of CE evolution a pair of white dwarfs separated by only a few  $R_{\odot}$  remain. Gravitational radiation losses eventually bring the pair closer until the smaller mass star begins to fill its Roche lobe. The minimum period (at contact) of such a system depends on the details of the constituents, but it may be as short as 5-6 minutes (Tutukov & Yungelson 1996; Hils & Bender 2000).

Theoretical studies by Tutukov & Yungelson (1996) and more recently, Nelemans et al. (2001) suggest that as many as  $\sim 10^8$  double-degenerate systems may populate the Galaxy. Because of their compact nature, these objects are ideal targets for space based gravitational wave detection with the Laser Interferometer Space Antenna (LISA) mission. They are likely the progenitors of at least some type Ia supernovae and may also represent a substantial fraction of supersoft X-ray sources (see Hils & Bender 2000; Nelemans, Yungelson & Portegies Zwart 2001). Their evolution has also been proposed as a channel for production of millisecond radio pulsars via accretion induced collapse (see Savonije, de Kool, & van den Heuvel 1986). An understanding of their formation, evolution and properties is therefore crucial to many areas of active astrophysical investigation.

The recent discovery of two double-degenerate binary candidates, RX J1914.4+2456 with a period of 569 s, and RX J0806+15 with a period of 321 s, has sparked keen interest in these objects (see Israel et al. 1999; Israel et al. 2002; Ramsay, Hakala & Cropper 2002). RX J1914.4+2456 (hereafter RX J1914) was discovered in the ROSAT all-sky survey. Motch et al. (1996) found that the X-ray flux is modulated with a period of  $\approx 569$  s, and concluded that the source was likely an intermediate polar (IP), with the 569 s period reflecting the spin period of the white dwarf primary. However, subsequent ROSAT observations did not find any additional periods such as are commonly present in IPs. This, combined with the unusual 100% X-ray modulation, led Cropper et al. (1998) to suggest that the source is a double-degenerate polar. Polars, systems containing an accreting strongly magnetized white

dwarf, rotate synchronously with the orbital period. If this identification is correct, RX J1914 has one of the shortest binary orbital periods known. If the orbital period is 569 s, and the secondary fills its Roche lobe, it must be a helium star, and perhaps a degenerate He white dwarf. Savonije et al. (1986) predict a minimum period of 636 s for a non-degenerate helium burning secondary, which, given the theoretical uncertainties, may not be long enough to completely rule out a non-degenerate secondary as argued by Cropper et al. (1998).

The X-ray spectrum of RX J1914 is soft, with a 40 eV blackbody model providing an acceptable fit to the ROSAT PSPC data (Motch et al. 1996; Cropper et al. 1998). The X-ray luminosity is in the range  $4 \times 10^{33}$  to  $1 \times 10^{35}$  ergs s<sup>-1</sup> for an assumed distance of 100 to 400 pc. Accretion at a rate of  $\sim 1 \times 10^{-8} M_{\odot}$  yr<sup>-1</sup> could conceivably power the X-ray flux. Ramsay et al. (2000) detected the optical counterpart to RX J1914. It is modulated in the V, R, and I bands at the 569 s period, but the optical peak leads the X-ray peak by about 0.4 cycles. This strengthens the orbital identification for the 569 s period. No other periods are seen in the optical data. More recent spectroscopy by Ramsay et al. (2002) reveals a line-free spectrum and no detectable polarization, inconsistent with its identification as a polar. If the source is indeed a polar, then the lack of polarization and emission lines is puzzling. Alternatively, Marsh & Steeghs (2002) have recently suggested that the primary may be non-magnetic and accretion takes place via direct impact of the accretion stream (ie. a double-degenerate Algol). An alternative not requiring accretion has been proposed by Wu et al. (2002). They suggest the system might be a unipolar inductor, with the secondary moving through the magnetic field of the primary because of a small asynchronism between the orbit and primary spin (in analogy with the Jupiter - Io system). This sets up an electric field which can drive currents in the magnetosphere, providing the energy for the X-ray emission.

Without any additional information it is difficult to determine which, if any, of the current hypotheses regarding the nature of RX J1914 is correct. However, strong clues to the nature of the X-ray flux could be obtained if the orbital evolution of the system can be detected. Indeed, for conservative mass transfer it is relatively straightforward to show that if the donor star is a degenerate dwarf, then stable mass transfer can only proceed with a widening of the orbit and a decrease in the orbital frequency (see Nelemans et al. 2001; Savonije et al. 1986). Thus, a measurement of the rate of change of the orbital frequency can provide a way to break the model degeneracy outlined above.

This possibility has led us to reinvestigate the available timing data on RX J1914, with the goal of trying to detect or constrain orbital frequency changes in the system. Here we report the results of our timing analysis of the ROSAT observations of RX J1914 over a period of  $\approx 4$  years. We find strong evidence for an increase in the orbital frequency of the

system at a rate of  $\approx 1.5 \times 10^{-17} \text{ Hz s}^{-1}$ , which is strikingly similar to that predicted by the loss of angular momentum due to gravitational radiation. The plan of this paper is as follows. In §2 we describe in detail our phase coherent timing study of the ROSAT data. We show that all the data can be phase connected and that a positive  $\dot{\nu}$  is strongly indicated. In §3 we discuss the implications of our findings for the nature of the X-ray emission from RX J1914 and show that orbital decay argues against accretion as the source of the X-ray flux unless the donor is non-degenerate. We conclude in §4 with a summary of our principle findings and plans for continued precision timing of such objects, and the synergy of such measurements with future space-based gravitational wave detection.

## 2. Data Extraction and Analysis

A total of  $\approx 80$  ksec of observing time on RX J1914 was obtained with ROSAT over the period from September, 1993 to October, 1997. Of the five observations, one was with the Position Sensitive Proportional Counter (PSPC), and the other four were High Resolution Imager (HRI) pointings. These data are now all in the public ROSAT archive. A number of studies of some or all of these data have been presented in the literature. Motch et al. (1996) discovered the 569 s modulation. Cropper et al. (1998) and Ramsay et al. (2000) have also reported timing results for RX J1914. Ramsay et al. (2000) used all the available ROSAT data, in addition to a single ASCA pointing and found that they could phase-connect all the data to within  $\approx 0.02$  cycles using a constant orbital frequency.

Table 1 gives a log of the observations used in our study. We used the HEASARC FTOOLS data analysis package (ie. XSELECT) to extract and analyse the data. We began by producing images and extracting source photons from a  $12''$  circle around the source centroid. In all cases the point source was easily identified and there were no source confusion problems. For example, Figure 1 shows the HRI image obtained from the April 30, 1996 observation (26 ksec exposure).

We next applied barycentric corrections to the photon times for each observation. We used the standard *bct* and *abc* ftools in conjunction with the ROSAT orbital and JPL (DE200) solar system ephemerides. We used the source coordinates ( $\alpha = 19^h 14^m 26.1^s$ ,  $\delta = 24^\circ 56' 43.6''$  :J2000) obtained by Ramsay et al. (2002) from their study of the optical-infrared counterpart to RX J1914. The ROSAT tool *abc* corrects for both the spacecraft clock drift and transforms to the barycentric frame. With the clock drift removed, the ROSAT clock is typically stable to a few 10s of milliseconds. Even a clock error of 100 milliseconds between observing epochs corresponds to only a  $1.8 \times 10^{-4}$  cycle error for RX J1914. Thus, the ROSAT times are more than precise enough for our purposes. Our extraction of source photons from the

five observations resulted in a total event list of 3,985 photons.

## 2.1. Coherent Timing Method

We performed a coherent timing analysis on the photon events using the  $Z_n^2$  statistic (Buccheri 1983; see also Strohmayer & Markwardt 2002 for an example of the use of this statistic in a similar context). In our study we performed model fitting in two complementary ways; a total power method based on the familiar  $Z_n^2$  (or Raleigh’s) statistic, and a phase fitting method similar to those used in pulsar timing studies.

For the total power method we evaluate;

$$Z_n^2 = \frac{2}{N} \sum_{k=1}^n \left[ \left( \sum_{j=1}^N \cos k\phi_j \right)^2 + \left( \sum_{j=1}^N \sin k\phi_j \right)^2 \right], \quad (1)$$

where;  $\phi_j = 2\pi \int_0^{t_j} \nu(t') dt$ ,  $\nu(t')$  is the frequency evolution model,  $t_j$  are the observed X-ray event times,  $N$  is the total number of X-ray events, and  $n$  counts the number of harmonics included in the sum. With this method we vary the timing model parameters in order to maximize the total power.

For our phase residual analysis we begin by defining the complex vector

$$C_n = \sum_{k=1}^n \left( \sum_{j=1}^N \cos k\phi_j + i \sum_{j=1}^N \sin k\phi_j \right). \quad (2)$$

The phase angle,  $\psi$  is then defined as

$$\psi = \tan^{-1} \left[ \frac{\sum_{k=1}^n \sum_{j=1}^N \sin k\phi_j}{\sum_{k=1}^n \sum_{j=1}^N \cos k\phi_j} \right]. \quad (3)$$

To perform the phase residual fit we break up the X-ray event times into a set of  $M$  bins and compute the phase angle  $\psi_l$  for each bin. The phases are simply given by;

$$\psi_l = \tan^{-1} \left[ \frac{\sum_{k=1}^n \sum_m \sin k\phi_m}{\sum_{k=1}^n \sum_m \cos k\phi_m} \right], \quad (4)$$

where the index  $m$  runs over all events in bin  $l$ . We can then compute

$$\chi^2 = \sum_{l=1}^M (\psi_l - \psi_{avg})^2 / \sigma_{\psi_l}^2, \quad (5)$$

where  $\psi_{avg}$  is the average phase angle computed from all  $M$  bins. We then minimize  $\chi^2$  to find the best fitting model. For a coherent signal the error  $\sigma_{\psi_i}$  in the phase angle is given simply by  $1/\sqrt{Z_n^2}$ .

In modelling the ROSAT event times we use a two parameter frequency model;  $\nu(t) = \nu_0 + \dot{\nu}(t - t_0)$ , where  $\nu_0$ ,  $\dot{\nu}$  and  $t_0$  are the orbital frequency at  $t_0$ , the orbital frequency derivative, and the reference epoch, respectively. With this model the phase advance due to  $\dot{\nu}$  has the well known quadratic time dependence;  $\Delta\phi = \frac{1}{2}\dot{\nu}(t - t_0)^2$ . To find the best model we jointly maximize the total  $Z_n^2$  power and minimize the phase residuals.

## 2.2. Theoretical Expectations

For a detached binary with a circular orbit the rate of change of the orbital frequency due to gravitational radiation is (see for example, Evans, Iben & Smarr 1987; Taylor & Weisberg 1989)

$$\dot{\nu}_{gr} = 1.64 \times 10^{-17} \left( \frac{\nu}{10^{-3} \text{ Hz}} \right)^5 \left( \frac{\mu}{M_\odot} \right) \left( \frac{a}{10^{10} \text{ cm}} \right)^2 \text{ Hz s}^{-1}, \quad (6)$$

where,  $\nu$ ,  $\mu$ , and  $a$  are the orbital frequency, reduced mass and orbital separation of the components, respectively. Given the 569 s orbital period of RX J1914, and likely scenarios for the binary components, a reduced mass of  $\mu \approx 0.05 M_\odot$  is likely (see Cropper et al. 1998; Wu et al. 2002). With these numbers we have  $\dot{\nu}_{gr} \approx 1.4 \times 10^{-17}$ . This  $\dot{\nu}$  would produce a total phase advance of  $\approx 0.1$  cycles over the four year timespan of the ROSAT data. We note again that this is orders of magnitude larger than any anticipated errors associated with drift of the ROSAT clock.

As noted earlier orbital evolution involves the interplay between mass transfer and angular momentum loss to gravitational radiation. Indeed, for conservative mass transfer it is relatively straightforward to show that if the donor star is a degenerate dwarf, then stable mass transfer can only proceed with a widening of the orbit and a decrease in the orbital frequency (see Nelemans et al. 2001; Savonije et al. 1986). If there is no mass transfer then one would expect the orbit to decay (positive  $\dot{\nu}$ ). In either case the *magnitude* of the orbital evolution is set by  $\dot{\nu}_{gr}$  above.

## 2.3. Results

We first performed a total  $Z_n^2$  power search using the model described above. We searched in a frequency range around the known 0.00659 day (1.756 mHz) period reported by

Ramsay et al. (2000). We sampled with a resolution substantially finer than the anticipated frequency resolution of  $1/T$ , where  $T$  is the total timespan of the data (about 4 years). As a first test we set  $\dot{\nu} = 0$  and found the constant frequency which maximized the  $Z_n^2$  power. We found a best frequency of  $1.7562467 \times 10^{-3} \pm 2 \times 10^{-10}$  Hz, consistent with the result of Ramsay et al. (2000). We next varied  $n$  to determine how many harmonics to include in our full analysis. We found that the majority of the signal was in the fundamental and first harmonic, so for the remainder of our analysis we fixed  $n = 2$ . Figure 2 shows the  $Z_2^2$  power spectrum in the vicinity of our best period. Note the multiple side-lobe peaks which result from the sparse sampling (ie. time gaps). However, there is no ambiguity with regard to the correct frequency, as all the sub-peaks have significantly lower power. Indeed, the total  $Z_2^2$  power is consistent with the sum of the powers obtained by analysing each observation individually. We therefore conclude, in agreement with Ramsay et al. (2000) that all the observations can be phase connected, that is, there is no cycle count ambiguity. This is also consistent with our expectations above for the magnitude of the orbital frequency derivative, which should produce a phase drift of order 0.1 cycle, much less than a complete cycle.

We next performed our joint search using the full two parameter  $(\nu, \dot{\nu})$  model. We did a grid search around the best frequency found from our initial  $\dot{\nu} = 0$  search, and we sampled a range of  $\dot{\nu}$  from  $-1 \times 10^{-16}$  to  $1 \times 10^{-16}$  Hz s $^{-1}$ , large enough to encompass our theoretical expectations for the magnitude of the orbital frequency derivative (see §2.2 above). For each  $\nu - \dot{\nu}$  pair we calculated the total power  $Z_2^2$  statistic as well as the  $\chi^2$  statistic using the phase residuals. For the  $\chi^2$  search we made phase measurements in all the good time intervals which were at least 400 s long. This resulted in 51 phase measurements. Figure 3 shows our calculated maps of constant  $\Delta\chi^2$  (top) and  $\Delta Z_2^2$  (bottom) versus  $\nu$  and  $\dot{\nu}$ . The results are remarkably consistent with each other and strongly indicate a positive  $\dot{\nu} = 1.5 \times 10^{-17}$  Hz s $^{-1}$ . Our minimum  $\chi^2$  is 56.7, which for 49 dof is entirely acceptable. For  $\dot{\nu} = 0$  we have a  $\Delta\chi^2 = 25$ , which excludes  $\dot{\nu} = 0$  at a significance of  $3.7 \times 10^{-6}$ , better than  $4\sigma$ . Table 2 summarizes our best timing solution.

Figure 4 shows the phase residuals for our best  $\chi^2$  timing solution. The abscissa is phase sample number (time ordered). The rms residual is 0.026 cycles and is indicated by the dotted horizontal lines. To further investigate the robustness of our solution we expanded the grid search in both  $\nu$  and  $\dot{\nu}$ . We did not find any other combinations of parameters which jointly maximized the  $Z_2^2$  power and minimized the phase residuals. We used our best fitting  $\chi^2$  model parameters to phase fold all the data. The resulting profile is shown in Figure 5. We compared this profile with those computed from each individual observation after phase folding with our best model, and found that they are all consistent within the errors. Figure 6 compares the folded profiles for each of the 5 observations listed in Table 1. The average profile using all the data is also shown as the bottom trace. Based on these comparisons it

seems unlikely that pulse profile variations could adversely influence the outcome of our fits.

## 2.4. Interpretation and Caveats

Previous optical timing studies of some CVs (including AM CVn itself) have proved problematic because of the possible presence of disk precession which can mimic and/or mask the true orbital period (see Patterson, Halpern & Shambrook 1993; Patterson et al. 1992 and references therein). Further, orbital period variations at the level of  $\Delta\nu/\nu \lesssim 1 \times 10^{-5}$  have been observed in a number of close binaries (see Warner 1988; Applegate 1992; and references therein). These variations, typically observed over timescales of decades or longer have been ascribed to magnetic activity of the low mass component (see Hall 1991; Applegate 1992; Arzoumanian, Fruchter & Taylor 1994). In particular, the presence of conditions necessary to produce a stellar dynamo, convection and differential rotation, appears to be essential for producing such variations (Applegate 1992). Applegate (1992) argues that the observed  $\Delta\nu/\nu$  can be produced by a change in the quadrupole moment of the active star. He argues that magnetic activity is the most likely process to account for the required changes in the mass quadrupole. If a change in the mass quadrupole is responsible for the observed orbital period variation in RX J1914, then it must have a magnitude  $\Delta q = (\dot{\nu}\Delta T/9\nu_0)(a/R)^2 \approx 4.3 \times 10^{-6}$ , where for simplicity we have assumed  $R$  is equal to the Roche lobe radius,  $R_L$ , and we have used the well known relation between orbital separation and the Roche lobe radius (see for example Paczynski 1967).

If RX J1914 is indeed a double-degenerate, then it would seem unlikely that such an effect could be responsible for the observed  $\dot{\nu}$ , however, for non-degenerate helium burning secondaries, a surface convection zone eventually forms (see Savonije et al. 1986), which might arguably support a dynamo and drive a magnetic activity cycle. However, it may be that all helium burning secondaries are excluded by reason of the 569 s orbital period (Savonije et al. 1986; Iben & Tutukov 1991). Such orbital period changes are also necessarily accompanied by substantial optical luminosity variations (of order 0.1 mag). Although there does not appear to be any direct evidence for such activity, and we regard this scenario as unlikely, we cannot at present definitively rule it out. One way to do so will be to obtain long term X-ray monitoring of the orbital period, as well as further optical - infrared monitoring. Such observations will test our ephemeris and, if confirmed, will enable a secure association of the observed  $\dot{\nu}$  with gravitational radiation. Another clue would come from a constraint on  $\ddot{\nu}$ . If the only torque acting is gravitational radiation, then it should have a characteristic magnitude  $\ddot{\nu} \approx 4 \times 10^{-31} \text{ Hz s}^{-2}$ . If a  $\ddot{\nu}$  term much greater than this is detected, then it will indicate the presence of additional torques in the system.



### 3. Implications and Discussion

As mentioned above, the orbital evolution has important implications for the nature of mass transfer in close binaries. If one assumes that the system angular momentum is dominated by the orbital motion, and if one also imposes the assumptions of conservative mass exchange and angular momentum loss only from gravitational radiation, then it is relatively straightforward to show that the orbital frequency derivative and mass accretion rate are given by the following expressions (see for example, Rappaport, Joss & Webbink 1982; Nelemans et al. 2001);

$$\dot{m}_2 = -1.72 \times 10^{-7} \left( \frac{m_2}{M_\odot} \right) \left( \frac{\mu}{M_\odot} \right) \left( \frac{a}{10^{10} \text{ cm}} \right)^2 \left( \frac{\nu}{10^{-3} \text{ Hz}} \right)^4 \left( \frac{1}{\left( \frac{\xi(m_2)}{2} + \frac{5}{6} - q \right)} \right) M_\odot \text{ yr}^{-1}, \quad (7)$$

and

$$\dot{\nu} = -8.21 \times 10^{-18} \left( \frac{\mu}{M_\odot} \right) \left( \frac{a}{10^{10} \text{ cm}} \right)^2 \left( \frac{\nu}{10^{-3} \text{ Hz}} \right)^5 \left( \frac{\left( \frac{1}{3} - \xi(m_2) \right)}{\left( \frac{\xi(m_2)}{2} + \frac{5}{6} - q \right)} \right) \text{ Hz s}^{-1}. \quad (8)$$

Here,  $m_2$  is the mass of the donor star,  $q \equiv m_2/m_1$  is the mass ratio ( $q < 1$ ), and  $\xi(m_2) = \frac{m_2}{r} \frac{dr}{dm_2}$ , is the dimensionless derivative of the radius of the donor  $r$ , with respect to its mass. From equation (7) one can see that for stability we need,  $\frac{\xi(m_2)}{2} + \frac{5}{6} > q$ . For stable mass transfer the only way to have  $\dot{\nu} > 0$ , as observed, is for  $\xi(m_2) > 1/3$ . This rules out degenerate donors since these stars grow as they lose mass and  $\xi(m_2) < 0$ .

If the orbital decay results only from gravitational radiation losses and there is no mass transfer, then the constraint on  $\dot{\nu}$  implies a constraint on the so called “chirp mass,”

$$\left( \frac{M_{ch}}{M_\odot} \right)^{5/3} = \left( \frac{\mu}{M_\odot} \right) \left( \frac{m_1 + m_2}{M_\odot} \right)^{2/3} = 2.7 \times 10^{16} \left( \frac{\nu}{10^{-3} \text{ Hz}} \right)^{-11/3} \dot{\nu}. \quad (9)$$

We show in Figure 7 the mass constraint derived from our  $\dot{\nu}$  measurement. The solid contour denotes the constraint for our best fit, while the dashed contours mark the  $1\sigma$  confidence limits. The inferred component masses are similar to those deduced by other researchers (see Ramsay et al. 2000; Wu et al. 2002; Marsh & Steeghs 2002).

#### 3.1. The Nature of the X-ray Flux

If the orbital frequency is indeed increasing, then this constrains models for the X-ray flux. If accretion powers the X-ray flux, then the mass - radius relation of the donor must be

such that the radius decreases as the mass drops (as for a non-degenerate, helium burning donor). If the system is accreting, then degenerate donors are excluded, at least within the confines of the conservative mass exchange assumptions. Our measurement of a positive  $\dot{\nu}$  favors a non-degenerate donor, although the observed orbital period is perhaps too short compared to theoretical predictions for the minimum period (of order 10 minutes) attainable by such systems (see Nelemans et al. 2001; Iben & Tutukov 1991).

Another alternative, proposed recently by Wu et al. (2002), is that the X-ray flux is powered by a unipolar inductor mechanism similar to that which is thought to operate between Jupiter and Io (Clarke et al 1996). In this model the donor sits inside its Roche lobe and no accretion takes place. In this case, both electrical and gravitational dissipation will cause the orbital frequency to increase, although gravitational losses dominate for most reasonable choices of the component masses (see Wu et al. 2002). Thus, this model is consistent with our  $\dot{\nu}$  measurement. A criticism of this model is that the lifetime of the unipolar inductor phase should be relatively short as synchronization should occur in  $\sim 1000$  yr (see Wu et al. 2002; Marsh & Steeghs 2002), unless some additional torque acts to hold the system out of synchronization. An example of a compact binary system which may be held out of synchronization is the “black widow” pulsar PSR B1957+20. This object shows orbital period variations somewhat similar to those seen in magnetically active close binaries (Arzoumanian, Fruchter & Taylor 1994). Applegate & Shaham (1994) suggest that a wind driven from the companion by pulsar irradiation drives a torque which acts to keep the system asynchronized. This leads to tidal dissipation which powers the companion and may also be responsible for the magnetic activity. Although this model does not appear directly applicable to RX J1914, it does suggest that other processes can maintain asynchronism over long timescales.

Recently, Marsh & Steeghs (2002) have proposed that RX J1914 is a “double-degenerate Algol,” accreting by direct impact of the accretion stream onto the primary. They argue that this model strongly favors a double-degenerate scenario for formation of AM CVn systems. In this model the components are not magnetized and the spins are not necessarily synchronized, however, the X-ray source associated with impact of the stream is fixed in the orbit frame. A positive  $\dot{\nu}$  argues against this scenario for RX J1914 unless the donor is non-degenerate because stable accretion with a degenerate donor implies a widening of the orbit (decreasing orbital frequency). A degenerate donor might still be viable if the mass transfer has gone unstable and formed a common envelope which is responsible for the observed orbital decay. However, this would appear to suffer from the same problem as the unipolar inductor model, that is, the lifetime of this phase would be short, moreover, at some point the X-ray flux would be obscured by the envelope. If more complete theoretical investigations firmly rule out all non-degenerate donors because of the short orbital period

then our positive  $\dot{\nu}$  measurement would provide strong evidence for a unipolar induction mechanism for RX J1914.

Although the interpretation of the 569 s period as the orbital period seems the most plausible, it is conceivable that the observed period is the spin period of an intermediate polar (IP), and that the orbital period has simply not been detected yet. If the system is an IP, then one would expect the orbital period to be longward of the 569 s spin period. Empirically, the spin and orbital periods of IPs satisfy  $P_{orb} \approx 10P_{spin}$ , so that a an orbital period  $\approx 100$  minutes is not unreasonable if RX J1914 is an IP. A mass donor in such a system would have a mass  $\approx 0.1M_{\odot}$ , implying an orbital separation,  $a \approx 1R_{\odot}$ . Such an orbit would introduce a phase delay to the white dwarf spin of at most a few seconds, which is much smaller than the phase offset implied for our best fit  $\dot{\nu}$ , so that the orbital modulation of a putative white dwarf spin would be negligible. If the primary white dwarf is accreting then it will experience a characteristic spin-up torque of magnitude,

$$N = \dot{m} (G M r_m)^{1/2} , \quad (10)$$

where  $r_m$  is the radius at which the accreting matter gets attached to the magnetic field of the primary. This torque will produce a characteristic spin-up rate,

$$\dot{\nu} = 7.97 \times 10^{-17} \left( \frac{\dot{m}}{10^{-8} M_{\odot} \text{ yr}^{-1}} \right) \left( \left( \frac{M}{M_{\odot}} \right)^{-1} \left( \frac{R}{10^{-2} R_{\odot}} \right)^{-3} \right)^{1/2} , \quad (11)$$

where for simplicity we have assumed  $r_m$  is equal to the white dwarf radius,  $R$ . Interestingly, this  $\dot{\nu}$  is not far from the observed value and can be made consistent with a reasonable choice of  $\dot{m}$ .

Empirically, the spin and orbital periods of IPs satisfy  $P_{orb} \approx 10P_{spin}$ , so that an orbital period  $\approx 100$  minutes is not unreasonable if RX J1914 is an IP. A mass donor in such a system would have a mass  $\approx 0.1M_{\odot}$ , implying an orbital separation,  $a \approx 1R_{\odot}$ . Such an orbit would introduce a phase delay to the white dwarf spin of at most a few seconds, which is much smaller than the phase offset implied for our best fit  $\dot{\nu}$ , so that the orbital modulation of a putative white dwarf spin would be negligible.

These considerations suggests an alternative possibility, that we are seeing the spin-up of an accreting white dwarf. A test of this hypothesis would be to make deeper searches for an as yet unseen orbital period longward of the 569 s observed period. Such a search would ideally be made by Chandra or XMM-Newton, whose wide, eccentric orbits will provide better sensitivity than previous satellites hampered by the nature of the low Earth orbit observing window. Although less likely than the orbital interpretation, if confirmed it would represent the first direct detection of the accretion induced spin-up of a white dwarf.

### 3.2. Gravitational Waves

The compact nature of RX J1914 makes it a prime source of gravitational radiation for space based detection. Its gravitational wave frequency  $2\nu_{orb} = 3.51$  mHz is within the most sensitive frequency range of the proposed LISA interferometer (see Armstrong, Estabrook & Tinto 2001), and is at high enough frequency to be outside the likely source confusion band produced by Galactic compact binaries (see Nelemans, Yungelson & Portegies Zwart 2001). The inferred strain amplitude for such systems,  $\approx 1 \times 10^{-21}$ , is well above the predicted LISA noise floor at this frequency.

If our timing solution is correct, then the phase advance due to  $\dot{\nu}$  is approaching 0.6 cycles, which can be easily confirmed with continued X-ray timing of the system, for example, with Chandra and XMM-Newton. If confirmed such observations will provide a much more accurate measurement of  $\dot{\nu}$ . Future monitoring will also establish if the observed  $\dot{\nu}$  is related to the orbital period variations seen in magnetically active binaries.

The combination of future X-ray timing and direct gravitational wave measurements would provide a powerful new probe of gravitational radiation and binary evolution. The X-ray measurements will directly aid future detection of the system by space-based interferometers, such as LISA. Measurement of the orbital frequency derivative combined with detection from space of the time dependence of the gravitational wave amplitude will provide the source distance (Schutz 1996). Moreover, the direct measurement of both orbital decay and the gravitational wave luminosity will provide new insights into the dynamics of orbital evolution in close binaries.

### 3.3. Summary

We have presented strong evidence that the 1.756 mHz X-ray frequency of RX J1914 is increasing at a rate of  $1.5 \times 10^{-17}$  Hz s<sup>-1</sup>. This rate is consistent with that expected from gravitational radiation losses in a detached compact binary and close to that expected given the likely scenarios which have been presented for the constituent masses of RX J1914. If the system were accreting from a degenerate donor, then one would naively expect the orbit to be widening and the frequency decreasing, in conflict with the observations. This suggests that accretion may not power the X-ray flux, as proposed recently by Wu et al. (2002), who suggest a unipolar induction mechanism as the source of the X-rays. Alternatively, a non-degenerate, helium burning secondary would be consistent with the observed  $\dot{\nu}$ , however, it may be that such systems cannot achieve such a short orbital period. Although we favor the gravitational radiation orbit decay interpretation, other compact, magnetically

active binaries have shown orbital period variations at a level similar to the implied orbital frequency change in RX J1914. It will have to wait for future monitoring of the orbit to completely rule out this possibility.

We thank Richard Mushotzky, Zaven Arzoumanian, Jean Swank and Craig Markwardt for many helpful comments and discussions. The work made use of data obtained from the High Energy Astrophysics Science Archive Research Center (HEASARC) at Goddard Space Flight Center.

### References

- Armstrong, J. W., Estabrook, F. B. & Tinto, M. 2001, *Class. and Quantum Gravity*, 18, 4059
- Arzoumanian, Z., Fruchter, A. S. & Taylor, J. H. 1994, *ApJ*, 426, L85
- Applegate, J. H. 1992, *ApJ*, 385, 621
- Applegate, J. H. & Shaham, J. 1994, *ApJ*, 436, 312
- Barrett, P., O'Donoghue, D., & Warner, B. 1988, *MNRAS*, 233, 759
- Buccheri, R. et al. 1983, *A&A*, 128, 245
- Clarke, J. T. et al. 1996, *Science*, 274, 404
- Cropper, M. et al. 1998, *MNRAS*, 293, L57
- Evans, C. R., Iben, I. & Smarr, L. 1987, *ApJ*, 323, 129
- Hall, D. S. 1991, *ApJ*, 380, L85
- Hils, D. & Bender, P. L. 2000, *ApJ*, 537, 334
- Iben, I. & Tutukov, A. V. 1991, *ApJ*, 370, 615
- Israel, G. L. et al. 1999, *A&A*, 349, L1
- Israel, G. L. et al. 2002, *A&A*, submitted (astro-ph/0203043)
- Marsh, T. R. & Steeghs, D. 2002, *MNRAS*, in press, (astro-ph/0201309)
- Motch, C. et al. 1996, *A&A*, 307, 459
- Nelemans, G., Yungelson, L. R., & Portegies Zwart, S. F. 2001, *A&A*, 375, 890
- Nelemans, G., Portegies Zwart, S. F., Verbunt, F. & Yungelson, L. R. 2001, *A&A*, 368, 939

- Patterson, J., Halpern, J. & Shambrook, A. 1993, ApJ, 419, 803
- Patterson, J., Sterner, E., Halpern, J. & Raymond, J. C. 1992, ApJ, 384, 234
- Ramsay, G., Cropper, M., Wu, K., Mason, K. O., & Hakala, P. 2000, MNRAS, 311, 75
- Ramsay, G., et al. 2002, MNRAS in press, (astro-ph/0202281)
- Ramsay, G. Hakala, P. & Cropper, M. 2002, MNRAS, submitted (astro-ph/0203053)
- Rappaport, S., Joss, P. C. & Webbink, R. F. 1982, ApJ, 254, 616
- Savonije, G. J., de Kool, M. & van den Heuvel, E. P. J. 1986, A&A, 155, 51
- Schutz, B. F. 1996, Class. and Quantum Gravity, 13, A219.
- Strohmayer, T.E., & Markwardt, C.B., 1999, ApJ, 516, L81
- Taylor, J. H. & Weisberg, J. M. 1989, ApJ, 345, 434
- Tutukov, A., & Yungelson, L. 1996, MNRAS, 280, 1035
- Warner, B. 1995, *Cataclysmic Variable Stars*, Cambridge Univ. Press, Cambridge UK.
- Wu, K. Cropper, M., Ramsay, G. & Sekiguchi, K. 2002, MNRAS in press, (astro-ph/0111358)

### Figure Captions

Fig. 1.— A portion of the ROSAT HRI image of RX J1914.4+2456 from the 1996 April 30 observation.

Fig. 2.— Power density spectrum computed using the  $Z_2^2$  power statistic, and  $\dot{\nu} = 0$ . The multiple side-lobe peaks result from the sparse sampling (ie. temporal gaps) of the time series. However, the sampling is sufficient to resolve any cycle count ambiguities. That is, all the sub-peaks are significantly below the central peak.

Fig. 3.— Summary of the joint grid search for  $\nu$  and  $\dot{\nu}$ . Shown are maps of constant  $\Delta\chi^2 \equiv \chi^2 - \min(\chi^2)$  (top) and  $\Delta Z_2^2 \equiv \max(Z_2^2) - Z_2^2$  (bottom). Here,  $\nu_0 \equiv 1.7562460 \times 10^{-3}$  Hz. For  $\Delta\chi^2$  we show contours at 2.3, 4.61, 6.1, 9.21 and 15, which for 2 degrees of freedom corresponds to confidence levels of 68%, 90%, 95%, 99% and 99.95%. In each map the cross (asterisk) symbol denotes the best parameters deduced from the  $\chi^2$  ( $Z_2^2$ ) fits. The two results are clearly consistent with each other.

Fig. 4.— Phase residuals (cycles) using the best fit parameters from minimizing  $\chi^2$ . The rms residual level is denoted by the horizontal dotted lines.

Fig. 5.— Phase folded pulse profile obtained by folding all the data with our best  $\chi^2$  solution.

Fig. 6.— Phase folded pulse profiles for each individual observation, using our best  $\chi^2$  solution. Each profile has been normalized to an amplitude of 1 and has been shifted vertically by 1 for clarity. Each observation is labelled with its start date (see also Table 1).

Fig. 7.— Constraints on the component masses from our  $\dot{\nu}$  measurement. The solid curve denotes the constraint for the best fitting  $\dot{\nu}$ , and the dashed contours denote the  $1\sigma$  confidence interval. The constraint was derived assuming no mass transfer and gravitational radiation as the only angular momentum loss mechanism.

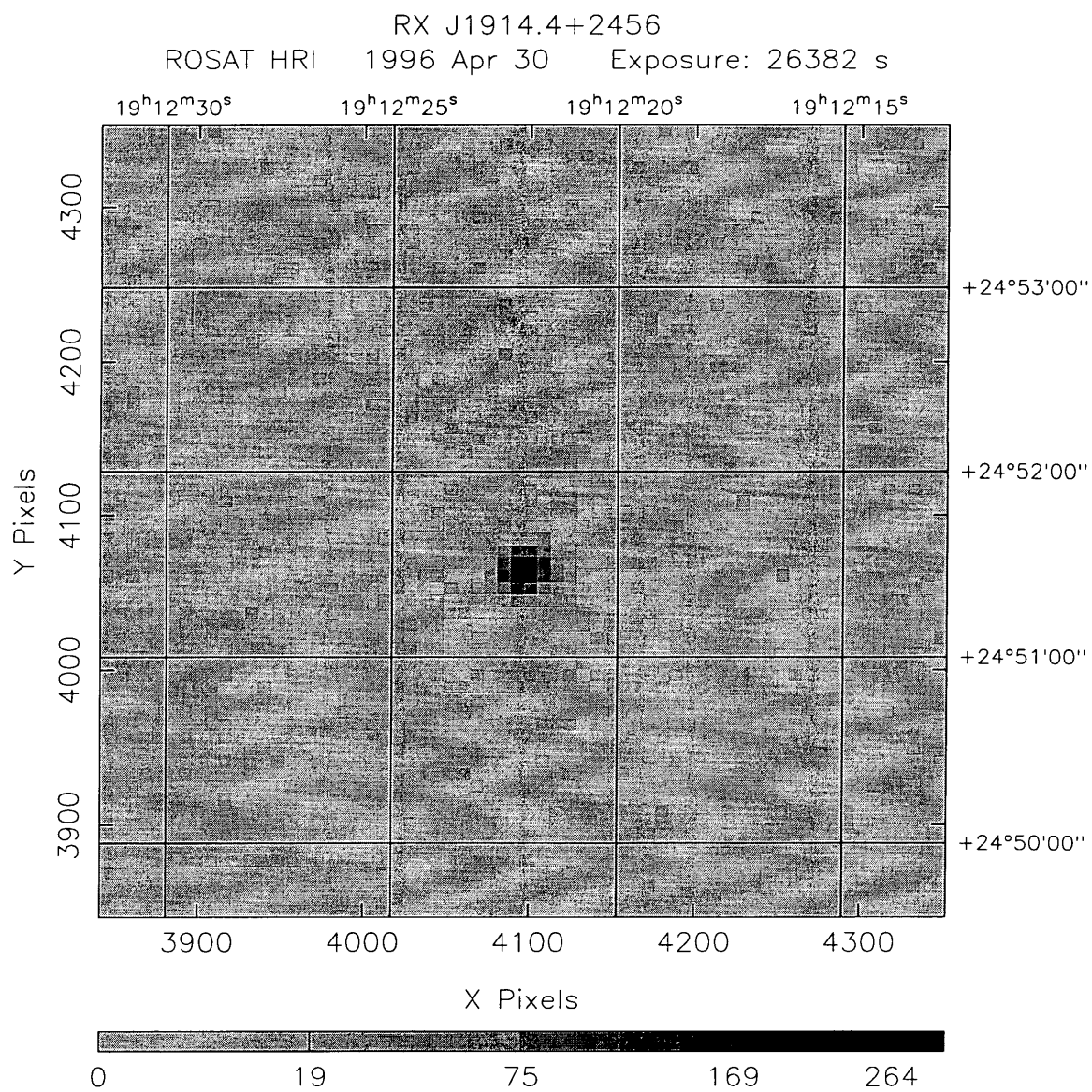


Figure 1: A portion of the ROSAT HRI image of RX J1914.4+2456 from the 1996 April 30 observation.



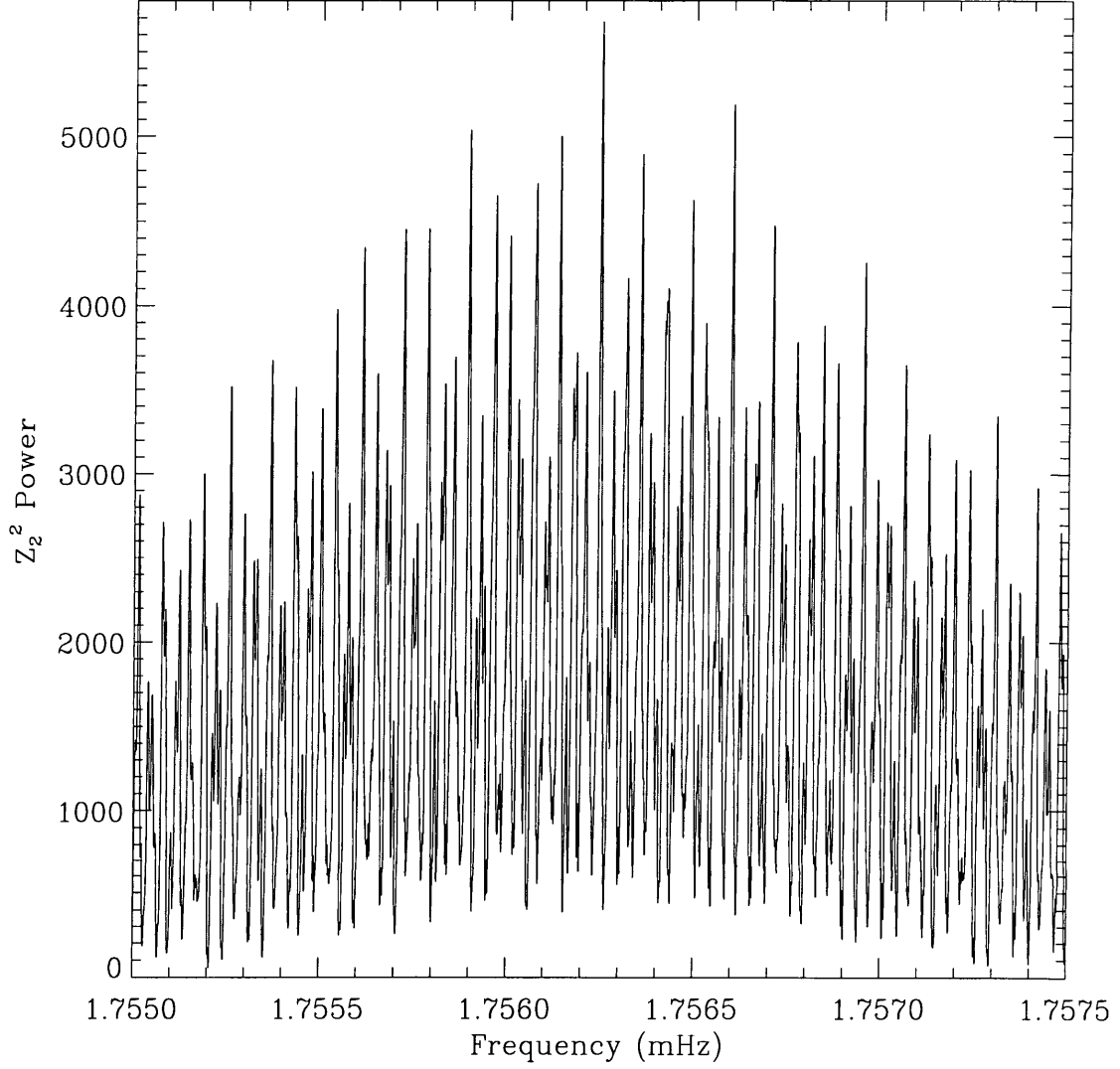


Figure 2: Power density spectrum computed using the  $Z_2^2$  power statistic, and  $\dot{\nu} = 0$ . The multiple peaks result from the sparse sampling (ie. temporal gaps) of the time series. However, the sampling is sufficient to resolve any cycle count ambiguities. That is, all the sub-peaks are significantly below the central peak.

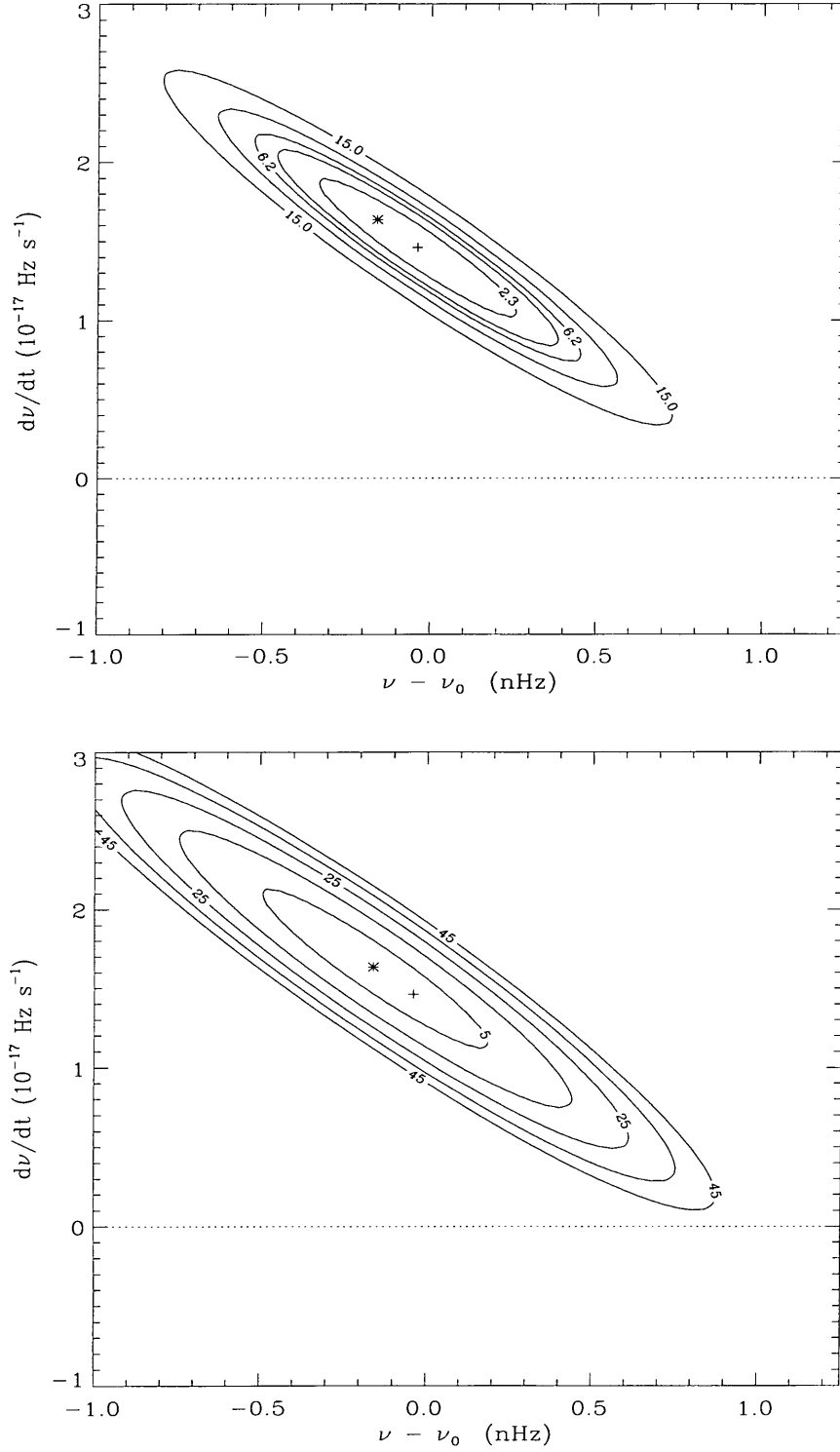


Figure 3: Summary of the joint grid search for  $\nu$  and  $\dot{\nu}$ . Shown are maps of constant  $\Delta\chi^2 \equiv \chi^2 - \min(\chi^2)$  (top) and  $\Delta Z_2^2 \equiv \max(Z_2^2) - Z_2^2$  (bottom). Here,  $\nu_0 \equiv 1.7562460 \times 10^{-3}$  Hz. For  $\Delta\chi^2$  we show contours at 2.3, 4.61, 6.1, 9.21 and 15, which for 2 degrees of freedom corresponds to confidence levels of 68%, 90%, 95%, 99% and 99.95%. In each map the cross (asterisk) symbol denotes the best parameters deduced from the  $\chi^2$  ( $Z_2^2$ ) fits. The two results

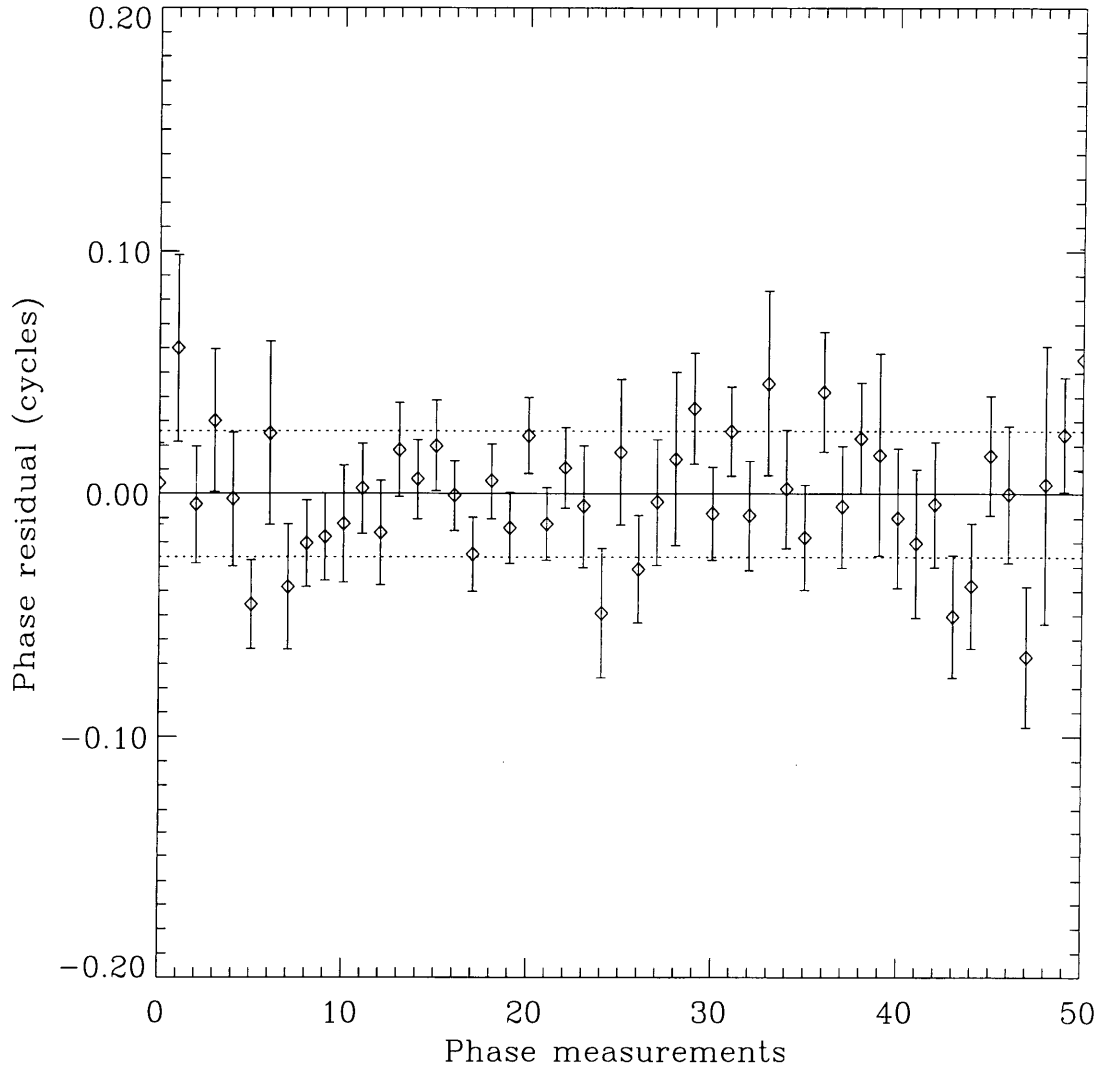


Figure 4: Phase residuals (cycles) using the best fit parameters from minimizing  $\chi^2$ . The rms residual level is denoted by the horizontal dotted lines.

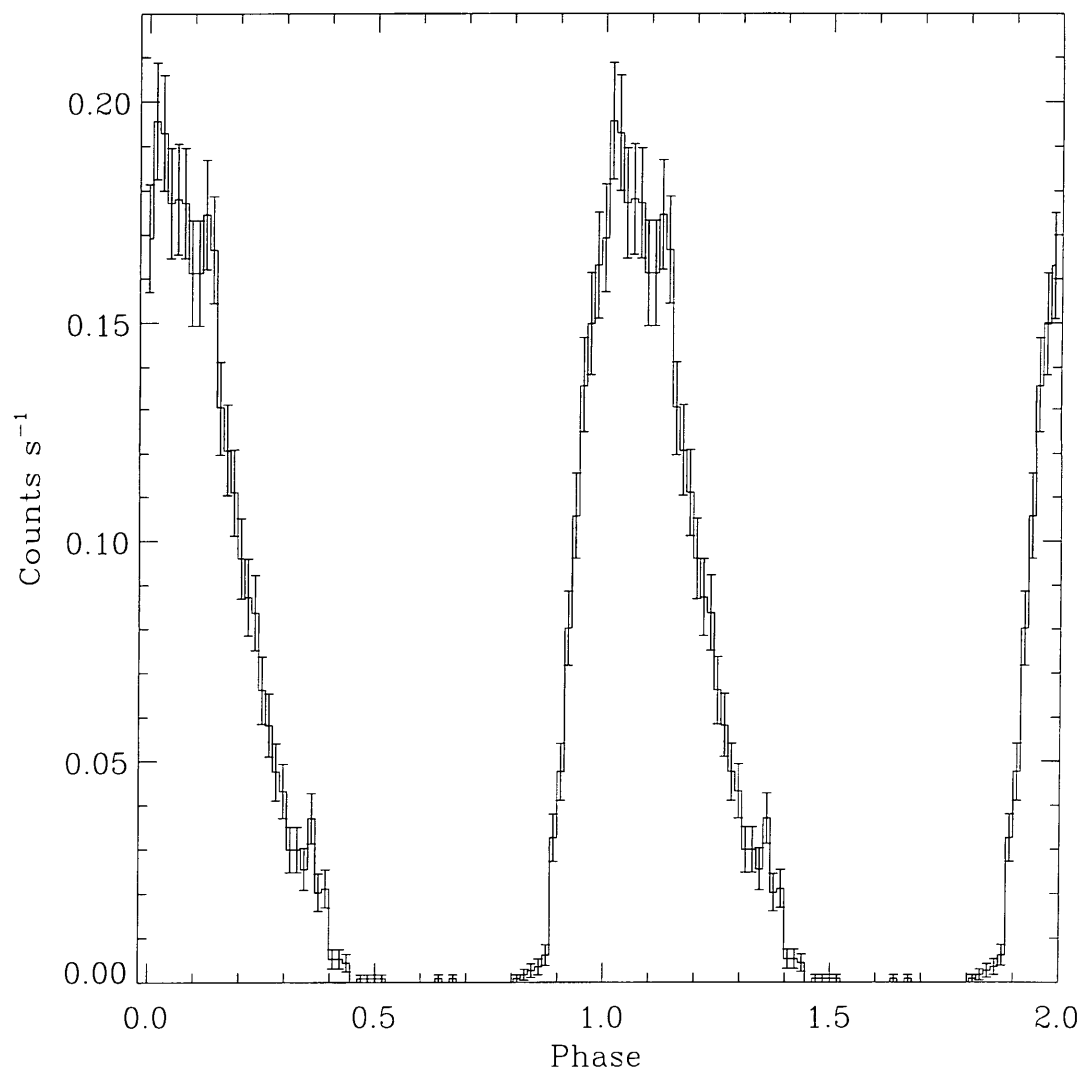


Figure 5: Phase folded pulse profile obtained by folding all the data with our best  $\chi^2$  solution.

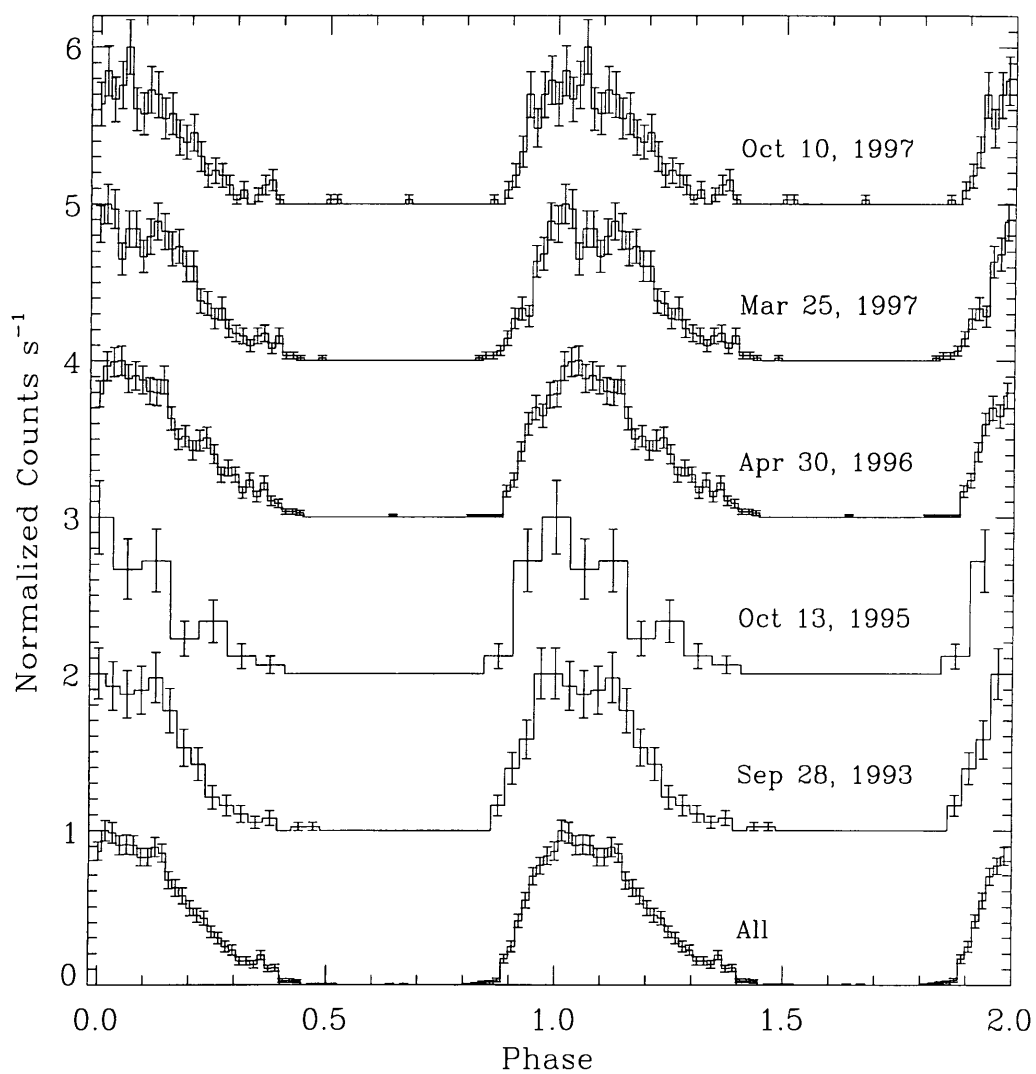


Figure 6: Phase folded pulse profiles for each individual observation, using our best  $\chi^2$  solution. Each profile has been normalized to an amplitude of 1 and has been shifted vertically by 1 for clarity. Each observation is labelled with its start date (see also Table 1).

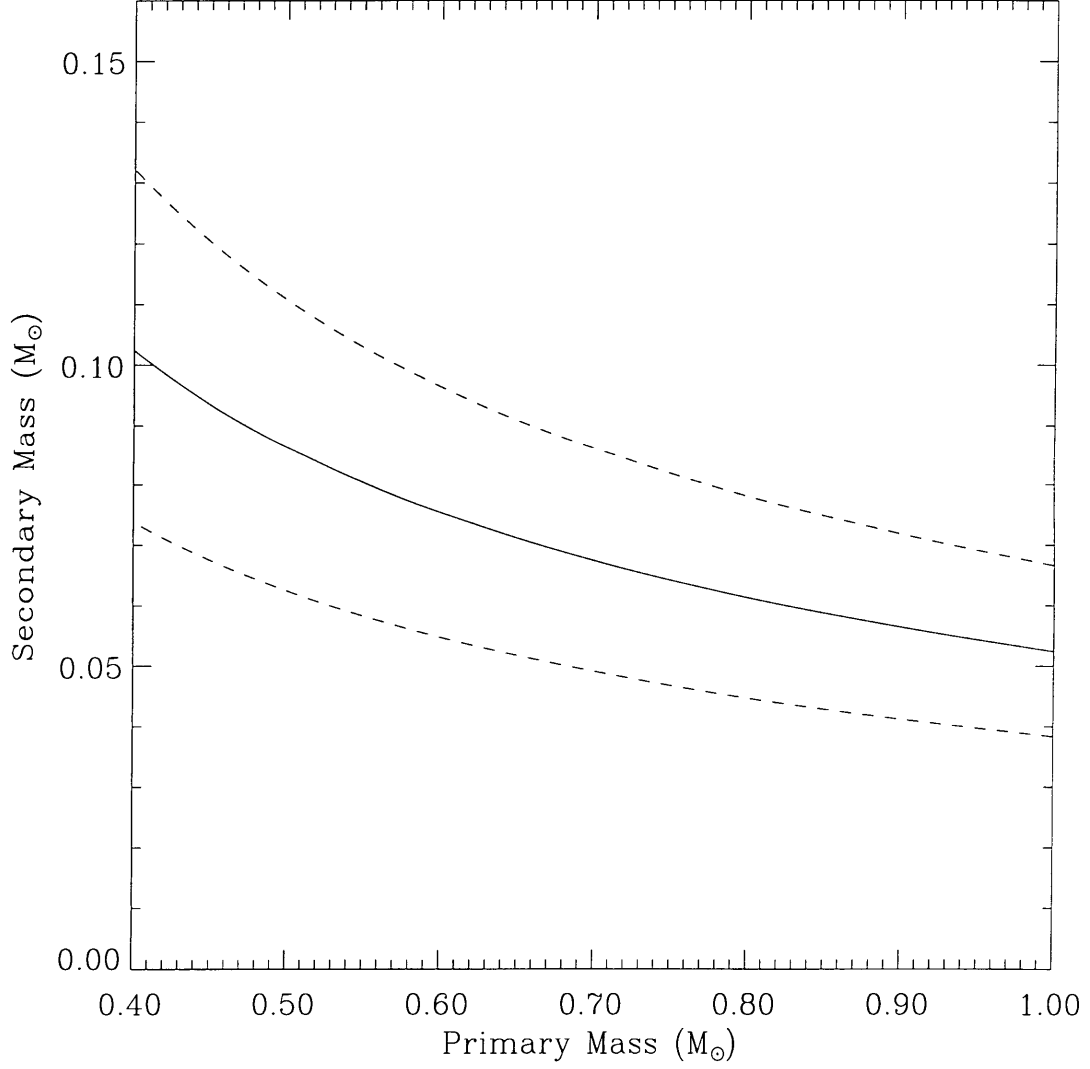


Figure 7: Constraints on the component masses from our  $\dot{\nu}$  measurement. The solid curve denotes the constraint for the best fitting  $\dot{\nu}$ , and the dashed contours denote the  $1\sigma$  confidence interval. The constraint was derived assuming no mass transfer and gravitational radiation as the only angular momentum loss mechanism.

Table 1: ROSAT Observations of RX J1914.4+2456

OBSID	Instrument	Start UT	Stop UT	Exposure (ks)
300337	PSPC	Sep 28, 1993	Sep 29, 1993	7.0
300509	HRI	Oct 13, 1995	Oct 13, 1995	2.4
300509	HRI	Apr 30, 1996	May 5, 1996	25.9
300587	HRI	Mar 25, 1997	Mar 28, 1997	19.4
300337	HRI	Oct 10, 1997	Oct 11, 1997	21.7

Table 2: Timing Solution for RX J1914.4+2456

Model Parameter	Value
$t_0$ (TDB)	49257.5333731 (MJD)
$\nu$ (Hz)	0.0017562459(3)
$\dot{\nu}$ (Hz s $^{-1}$ )	$1.5(4) \times 10^{-17}$

